varied to increase the ability of their detection. The neuronal holding potential was slowly swept from −50 to +34 mV, during which time MEPPs continued to be recorded at higher frequency. However, no MEPP-correlated single-channel currents were observed on the neuronal membrane.

Challenges to the idea of vesicular release of transmitter have supported the idea of the release of cytoplasmic transmitter. Using the favorable characteristics of cultured *Xenopus* nerve and muscle cells, we have examined a possible alternate mechanism, whereby cytoplasmic ACh is gated through channels in the neuronal membrane. We found no evidence for such channels, even when the amount of transmitter released was large. We would expect to observe such channels given the large size of the ACh molecule. ACh will not pass through the high conductance (60 pS) ACh-receptor channel, a channel whose permeability is relatively nonspecific to cations. This ACh-receptor channel is detectable in our system, but we detected no transmitter channel. The argument could be made that such a channel could be highly selective to the ACh cation, excluding other smaller and more abundant cations such as K^+ or Na^+, and thereby could have a much smaller conductance and escape detection.

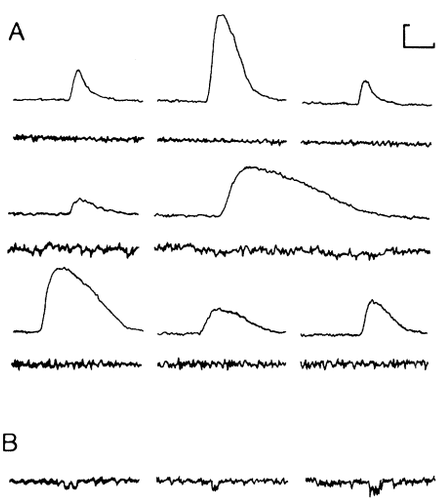

Fig. 2. (**A**) Simultaneous records of muscle membrane potentials and neuronal membrane currents during production of MEPPs. Each record consists of a pair of traces: the upper trace is muscle membrane potential, and the lower trace is neuronal membrane current. Records are presented from three separate nerve-muscle contacts. In no case were large single channels observed to open in the nerve membrane before, during, or after the MEPP. Scale bars, top: 5 mV, 25 pA, 20 msec; middle: 20 mV, 12.5 pA, 10 msec; bottom: 20 mV, 12.5 pA, 20 msec. (**B**) Single-channel openings on the neuronal membrane not correlated with MEPPs. These three channel openings occurred more than 200 msec before or after an MEPP on the muscle membrane. Scale bars: 12.5 pA; 20 msec, 10 msec, 10 msec.

To our knowledge, no channel with such very high selectivity to ACh has yet been described, although there is a report of a carrier, hexadecavalinomycin, that has a permeability to ACh that is 4.5 times as high as its permeability to K^+ (*5*).

Taken together, these arguments suggest that the amplitude of the current passing through presumptive neuronal membrane channels which regulate the release of ACh would be detectable by our technique, especially during the generation of a large MEPP. Thus, we conclude that it is very unlikely that such transmitter channels exist at the neuromuscular junction.

REFERENCES AND NOTES

1. M. Israel, Y. Dunant, R. Manaranche, *Prog. Neurobiol. (Oxford)* **13**, 237 (1979); L. Tauc, *Physiol. Rev.* **62**, 857 (1982); Y. Dunant and M. Israel, *Sci. Am.* **252**, 58 (April 1985); M. Israel *et al.*, *Proc. Natl. Acad. Sci. U.S.A.* **83**, 9226 (1986).
2. I. Chow and M.-m. Poo, *J. Neurosci.* **5**, 1076 (1985).
3. Y. Igusa and Y. Kidokoro, *J. Physiol. (London)* **389**, 271 (1987).
4. N. Patel and M.-m. Poo, *J. Neurosci.* **2**, 483 (1982).
5. G. Eisenman, S. Krasne, S. Ciani, in *Ion-Selective Electrodes and Enzyme Electrodes in Medicine and in Biology*, M. Kessler *et al.*, Eds. (Urban and Schwarzenberg, Munich, 1976), pp. 3–21.

6. We thank S. Hagiwara and A. D. Grinnell for helpful comments. Supported by NSF grants BNS 85-10794 and BNS 84-19893, and a grant from the Muscular Dystrophy Association to S.H.Y.

3 August 1987; accepted 5 November 1987

The Structure of Sister Minichromosome DNA Before Anaphase in *Saccharomyces cerevisiae*

DOUGLAS KOSHLAND* AND LELAND H. HARTWELL

The role of DNA topology in holding sister chromatids together before anaphase was investigated by analyzing the structure of a small circular minichromosome in cell cycle (cdc) mutants of the yeast *Saccharomyces cerevisiae*. In the majority of cells arrested after S phase but before anaphase, sister minichromosome molecules are not topologically interlocked with each other. The analysis of the ploidy of minichromosomes in cells that are released from arrest demonstrates that the sister molecules are properly segregated when the cell cycle block is removed. Therefore, sister minichromosome molecules need not remain topologically interlocked until anaphase in order to be properly segregated, and topological interlocking of sister DNA molecules apparently is not the primary force holding sister chromatids together.

SISTER CHROMATIDS ARE HELD TOgether from the time of their replication to the beginning of anaphase. This interaction is presumably essential to the mechanism that orients the segregation of two sister chromatids such that they segregate to opposite poles of the cell during anaphase. In addition, the ability of the cell to eliminate this interaction is essential for proper chromosome segregation in anaphase and in fact may be the primary event that initiates the onset of anaphase. Several models have invoked the topological interlocking of sister DNA molecules (by partially replicated centromere DNA or catenation) as the mechanism for holding sister chromatids together (*1–3*). In fact, at least some catenation of sister chromatids may exist before anaphase (*4, 5*). However, no one has determined the extent of topological interlocking between sister chromatids before anaphase or whether the persistence of these structures is essential for their proper segregation.

Department of Genetics SK50, University of Washington, Seattle, WA 98195.

*Present address: Department of Embryology, Carnegie Institution of Washington, Baltimore, MD 21210.

To begin the analysis of the structure of chromosomal DNA at different stages of the cell cycle, we analyzed the structure of the minichromosome, pDK243, in an asynchronous population of wild-type yeast (*Saccharomyces cerevisiae*) cells grown at 23°C and 36°C (Fig. 1). This minichromosome is approximately 14 kb long and contains a putative origin of replication (*ARS1*), a centromere (*CEN3*), and a modified form of the *ADE3* gene (*ade3*-2p), which allows the ploidy of the minichromosome to be monitored in individual cells (*6*). A plasmid-specific probe identifies three distinct bands (Fig. 1a, wt at 36°C) that are present only in plasmid-bearing cells. The majority of pDK243 DNA in asynchronous wild-type cells (at either temperature) is closed circular monomer (Table 1) by the criterion that the major band comigrates with closed circular monomers from *Escherichia coli*. A small fraction of the minichromosome DNA isolated from these cells comigrates with nicked monomers from *E. coli*; the nicked circular form may be present inside the yeast cell or may be produced by nicking during the DNA isolation procedure. Approximately 15% of the total minichromosome DNA migrates at a third position, band C. The

molecules in this band are probably C forms, two closed circular intertwined monomers (*7*), because their mobility relative to closed circular dimers of pDK243 (*8*) is similar to the mobility of C forms of SV40 relative to closed circular dimers of SV40 (*7*). In addition, the molecules of band C are superhelical, since conditions that promoted the extensive nicking of these molecules caused the disappearance of band C and the appearance of a new band of approximate equal intensity (band A), which migrated more slowly (Fig. 1a, *cdc9* at 36°C) as expected of two catenated nick circles (*7*). Finally, they exhibit a more heterogeneous mobility on gels lacking ethidium bromide (*8*) as expected if they contain a distribution of catenae (*37*).

A variety of stage-specific blocks produced by mutation (cdc) or by inhibitors have been defined in yeast with reference to the landmark events of the initiation of DNA synthesis, the completion of DNA synthesis, elongation of the spindle, nuclear division, and cytokinesis (*9–14*). To determine whether topological interlocks between sister minichromosome DNA persist before anaphase, we arrested cells containing the minichromosome at different stages of the cell cycle using cdc mutations or inhibitors and analyzed the structure of minichromosome DNA (see legend to Fig. 1). If topological interlocks between sister minichromosome molecules are responsible for holding them together until anaphase, then we would expect to see the majority of molecules interlocked with a sister molecule in cells arrested after S phase but before anaphase (*cdc13*, *cdc16*, *cdc20*, or nocodazole-treated) but not in cells arrested before the completion of S phase (*cdc28*, *cdc4*, *cdc7*, *cdc17*, *cdc2*, *cdc6*, *cdc9*, or hydroxyurea-treated) or after anaphase (*cdc14* or *cdc15*). The major structural form of minichromosome DNA found in cells arrested after S phase but before anaphase (Fig. 1b, at 36°C: *cdc13*, *cdc16*, *cdc20*, and nocodazole-treated) was closed circular monomer, as it was in cells arrested in other stages of the cell cycle except cells arrested by *cdc9* at 36°C (Fig. 1a). Since the in vivo structure of the minichromosome is apparently preserved during the isolation procedure (see below), the majority of sister minichromosomes do not remain intertwined with each other in cells arrested before anaphase.

A small amount of bands A and C (approximately 1 to 5%) was found in cells arrested in S phase (*cdc2*, *cdc9*, *cdc17*, and hydroxyurea-treated) or after S phase but before anaphase (*cdc13*, *cdc16*, *cdc20*, and nocodazole-treated); however, even in these cells the proportion of minichromosome DNA that is catenated is only a small percentage of the total. As proposed by Holm *et al.* (*5*) the persistence of a small amount of catenated dimers before anaphase can be explained by the fact that catenated sister molecules should be in equilibrium with noncatenated sister molecules, because the topoisomerase II reaction is reversible (*15*), and the concentration of sister DNA molecules is high before their segregation. The small percentage of catenated dimers in asynchronous cultures probably arose from the fraction of cells that were either in S phase or after S phase but before anaphase at the time of DNA isolation.

Three lines of evidence suggest that the DNA isolation procedure apparently preserved the structure of the minichromosome present in vivo in the arrested cells. First, the procedure inactivated nonspecific nucleases as evidenced by the preponderance of closed circular DNA in most preparations (Fig. 1 and Table 1). Second, minichromosome molecules migrated predominantly as nicked circles (Fig. 1a, *cdc9* at 36°C) in cells inactivated for the wild-type DNA ligase gene [*CDC9* (*16*)], and as topoisomers (Fig. 1b, *Top* II at 36°C) in cells inactivated for topoisomerase II [*TOP2* (*17*)] characteristic of the structures one would expect to exist in vivo. Third, the procedure immediately inactivated topoisomerase II as evidenced by the quantitative recovery of topoisomers of pDK243 DNA isolated from a mixture of wild-type cells and cells inactivated for topoisomerase II (*8*).

The biological significance of the closed circular monomers observed in cells arrested before anaphase could be judged by determining whether minichromosomes with this structure could be segregated with high fidelity to daughter cells when these arrested cells were allowed to recover. The fidelity of minichromosome transmission in the first division after recovery from arrest (Table 1) was determined by a color assay for chromosome ploidy (*6*). When either the fidelity of minichromosome transmission or the fraction of recovering cells is low (*cdc2*, *cdc6*,

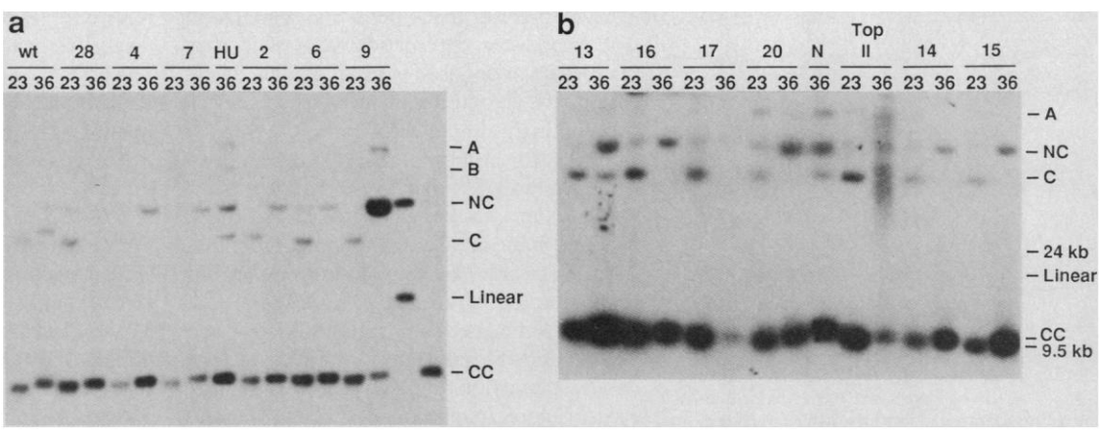

Fig. 1. A series of congenic strains were constructed that contained a selectable marker for transformation (*leu2*), the minichromosome pDK243 (*6*), mutations in the *ADE3* and *ADE2* genes, which allow one to follow the transmission of pDK243 during vegetative growth (*6*), and cdc mutants (*9*). Cells from wild-type and cdc strains were grown at 23°C to a density of 1×10^7 in YM-1 plus glucose; a portion of these cells was shifted to 36°C. In addition, hydroxyurea (0.1*M*) or nocodazole (100 μ*M*) was added to a portion of the wild-type cells. After 3 hours at 36°C, more than 90% of the cells accumulated with the specific terminal phenotype characteristic of the cdc mutation in the cells or the particular inhibitor. Minichromosome DNA was isolated (*25*) from cells grown at 23°C (just before the shift to 36°C) or after imposing the cell division cycle block for 3 hours. Two precautions were taken to preserve the structure of the minichromosome DNA that accumulated in cells arrested at 36°C. Minichromosome DNA was isolated from these cells in a 36°C room with prewarmed equipment and reagents so as to ensure constant temperature. Hydroxyurea or nocodazole was included in lysis reagents, when used. As a second precaution, diethyl pyrocarbonate was present in the lysis reaction. The DNA isolated from these cells was run on a 0.5% agarose gel in the presence of ethidium bromide, and minichromosome DNA was detected by DNA hybridization with pBR322 as probe. (**a**) Autoradiogram of a gel containing DNA from wild-type cells (wt) and cells containing cdc mutations (numerical designations are shown) growing asynchronously at 23°C or arrested at 36°C. HU, wild-type cells arrested by hydroxyurea. Unlabeled lanes represent standards. (**b**) Autoradiogram of a gel containing DNA from cells containing cdc mutations as designated in (a); N, wild-type cells arrested with nocodazole. DNA from cells containing a temperature-sensitive mutation in topoisomerase II was also isolated under conditions where the enzyme is active (23°C) and inactive (36°C). Position of migration of nicked circular monomer pDK243 (NC), closed circular monomer pDK243 (CC), linear monomer, and 9.5- and 24-kb λ Hind III bands are indicated. The structure of band B is unknown.

cdc7, *cdc9*, *cdc14*, *cdc15*, *cdc16*, and *cdc17*), it is impossible to assess whether the majority of minichromosomes in arrested cells are good substrates for subsequent transmission. However, when the fidelity of minichromosome transmission in recovering cells is high and the recovery of arrested cells is also high [cells arrested by *cdc28*, *cdc4*, or *cdc13* mutations or by the inhibitors, nocodazole and hydroxyurea (Table 1)], then the majority of minichromosomes in these arrested cells must be substrates that are capable of being efficiently transmitted to daughter cells. We conclude that the closed circular monomers of the minichromosome found in cells arrested by *cdc13* or nocodazole (after S phase but before anaphase) are capable of being transmitted to daughter cells with high efficiency.

The presence of only a small fraction of interlocked sister minichromosomes in cells blocked by *cdc13* mutations or nocodazole is supported by observations that suggest that the topological interlocks between sister molecules may be extremely transient during the cell cycle. Centromeric DNAs of at least some of yeast chromosomes (including *CEN3*) apparently replicate early in S phase (*18*), suggesting that topological interlocks as a consequence of partially replicated centromere DNA do not persist even until the end of S phase. In addition, the majority of interlocks between sister molecules that result from catenation are also apparently very transient (*7, 19*), probably because topoisomerase II activity is present in the cell cycle as early as S phase (*20*) and can remove most catenation between sister molecules immediately after they are formed.

Assuming that the segregation of sister chromatids in yeast is similar to the segregation of sister chromatids in other organisms, they must remain associated to each other before anaphase in order to segregate properly at anaphase. In particular, sister minichromosomes must have remained physically associated with each other in cells blocked before anaphase in order to segregate with high fidelity when the block was released. The failure to observe topological interlocks between the majority of sister minichromosomes in cells blocked before anaphase suggests that topological interlocks between sister minichromosomes are not an essential part of the mechanism that holds sister chromatids together in vivo. Though the conditions used in this study for the isolation and characterization of minichromosome DNA structure were sufficient to preserve the association of sister minichromosomes by topological interlocks had they existed, they were chaotropic for proteins and would have caused the dissociation of sister minichromosomes into monomers as observed. Thus it is reasonable to postulate the existence of one or more interesting proteins that function to hold sister chromatids together. In fact, several proteins have recently been discovered that are good candidates for holding sisters together, because they are positioned between the kinetochore and arms of the two sister chromatids before anaphase and then dissociate from the chromosomes during anaphase (*21*).

Whether the structure of minichromosomes before anaphase provides insights into the mechanism that holds sister chromatids together before anaphase depends on the assumption that the minichromosome mimics the behavior of endogenous chromosomes. The coincident effect of cis and trans mutations on the fidelity of transmission of minichromosomes and endogenous chromosomes suggests that these chromosomes require many, if not all, the same functions for their replication and segregation (*8*). Furthermore, the minichromosome used in this study is replicated and segregated properly in 99.3% of mitotic divisions (*6*); presumably the minichromosome must behave like endogenous chromosomes at most stages of the cell cycle to achieve such a high fidelity of transmission. While errors in minichromosome transmission are rare (7×10^{-3} per cell division), errors in endogenous chromosome transmission are even rarer [10^{-5} per cell division (*22, 23*)]. This difference in error rates could reflect that the minichromosome behaves differently from the endogenous chromo-

Table 1. Quantitative analysis of structural and genetic properties of minichromosome DNA isolated from cells arrested at specific stages of the cell cycle. The percent of minichromosome DNA in one of four conformational states was determined as follows. The intensity of each band within a lane of Fig. 1 was determined by scanning the lane with a soft laser densitometer. The percent of minichromosome DNA in a lane that migrates in a particular band was determined by dividing the intensity of that band by the sum of the intensities of all the bands in the lane. The number of viable cells in a culture just before shifting the culture to conditions that arrest the cells' progression through the cycle (C_0) and just before DNA isolation (C_a) were determined by titering the cells for colony-forming units. The expected number of viable cells in C_a if no cell death occurs in the culture prior to DNA isolation can be calculated from (C_0) and the fraction of cells in C_0 that divide once after the shift to the conditions promoting cell arrest (*24*). The percentage of viable cells at the time of DNA isolation was calculated by dividing the observed number of viable cells in C_a by the expected number of viable cells. The fidelity of minichromosome transmission was found from the color assay for monitoring minichromosome ploidy (*6*). The assay was used to determine first, the fraction of first divisions after recovery in which both daughter cells got one copy of the plasmid and second, the fraction of cells in the culture with one copy before arrest (*6*). The fraction of cells that contained one copy of the plasmid before arrest and then subsequently properly transmitted the minichromosome to the two daughter cells upon recovery from arrest was calculated by dividing the first fraction by the second. Abbreviations as in Fig. 1.

CDC	Temperature (°C)	Conformation of DNA (%)				Viability after arrest	Fidelity of minichromosome transmission (%)
		CC	NC	C	A		
wt	23	87	0	13	0		
	36	79	6	15	0	100	99
28	23	82	3	15	0		
	36	98	2	0	0	67	97
4	23	85	5	10	0		
	36	88	12	0	0	59	94
7	23	94	3	3	0		
	36	78	22	0	0	20	90
2	23	78	0	22	0		
	36	81	17	2	0	25	85
6	23	76	5	19	0		
	36	91	9	0	0	30	79
9	23	77	2	21	0		
	36	16	79	0	5	12	73
wt + HU	36	80	12	6	2	78	95
13	23	88	0	12	0		
	36	88	9	3	0	92	95
16	23	84	4	12	0		
	36	88	12	0	0	100	65
17	23	91	0	9	0		
	36	98	1	1	0	31	77
20	23	80	3	16	1		
	36	80	19	1	0		
wt + N	36	73	17	5	5	>80	97
Top II	23	87	2	11	0		
	36	23	0	0	0		86
14	23	84	6	10	0		
	36	95	5	0	0	29	64
15	23	92	0	8	0		
	36	95	5	0	0	32	93

some at some stage in every cycle. However, given that errors in minichromosome transmission are rare, it seems more likely that the minichromosome behaves differently than the endogenous chromosomes at some stage of the cell cycle in only a small fraction (0.7%) of the cell divisions.

REFERENCES AND NOTES

1. G. Tschumper and J. Carbon, *Gene* **23**, 221 (1983).
2. A. W. Murray and J. W. Szostak, *Annu. Rev. Cell Biol.* **1**, 289 (1985).
3. O. Sundin and A. Varshavksy, *Cell* **25**, 659 (1981).
4. T. Uemura and M. Yanagida, *EMBO J.* **5**, 1003 (1986).
5. C. Holm *et al.*, *Cell* **41**, 553 (1985).
6. D. Koshland *et al.*, *ibid.* **40**, 393 (1985).
7. O. Sundin and A. Varshavksy, *ibid.* **21**, 103 (1980).
8. D. Koshland and L. H. Hartwell, unpublished results.
9. J. R. Pringle and L. H. Hartwell, in *The Molecular Biology of the Yeast* Saccharomyces, *Life Cycle and Inheritance*, J. N. Strathern *et al.*, Eds. (Cold Spring Harbor Laboratory, Cold Spring Harbor, NY, 1981), pp. 97–142.
10. B. Byers and L. Goetsch, *Cold Spring Harbor Symp. Quant. Biol.* **38**, 123 (1973).
11. G. Brunborg and D. H. Williamson, *Mol. Gen. Genet.* **162**, 277 (1978).
12. F. Fabre, *Radiat. Res.* **56**, 795 (1976).
13. M. A. Resnick, *J. Theor. Biol.* **59**, 97 (1976).
14. J. V. Kilmartin, *Biochemistry* **20**, 3629 (1981).
15. T. Goto and J. C. Wang, *J. Biol. Chem.* **257**, 5866 (1982).
16. L. H. Johnston and K. A. Nasmyth, *Nature (London)* **274**, 891 (1978).
17. S. DiNardo, K. Voelkel, R. Sternglanz, *Proc. Natl. Acad. Sci U.S.A.* **81**, 2616 (1984).
18. R. McCarroll and W. Fangman, personal communication.
19. D. T. Weaver *et al.*, *Cell* **41**, 565 (1985).
20. S. J. Brill, S. DiNardo, K. Voelkel-Meiman, R. Sternglanz, *Nature (London)* **326**, 414 (1987).
21. C. A. Cooke *et al.*, *J. Cell Biol.*, in press.
22. L. H. Hartwell *et al.*, *Rec. Adv. Yeast Mol. Biol.* **1**, 28 (1982).
23. M. S. Esposito *et al.*, *Curr. Top. Genet.* **6**, 5 (1982).
24. L. H. Hartwell *et al.*, *Genetics* **74**, 276 (1973).
25. K. A. Nasmyth and S. I. Reed, *Proc. Natl. Acad. Sci. U.S.A.* **77**, 2119 (1979).

26. We thank J. Kent and L. Rutledge for technical assistance. We thank M. Carson, C. Holm, D. Burke, S. DiNardo, and A. Murray for valuable discussions. D.K. was a fellow of the Helen Hay Whitney Foundation and a Lucille P. Markey Scholar. This work was also supported by the Lucille P. Markey Charitable Trust, a grant from the Public Health Service (GM-17709) and a grant from the American Business Foundation for Cancer Research.

13 July 1987; accepted 15 October 1987

Intracellular Topography of Rhodopsin Bleaching

CLINT L. MAKINO,* LOUIS N. HOWARD, THEODORE P. WILLIAMS

In a vertebrate eye, the photoreceptor cells are aligned so that most of the light passes through them lengthwise. At the light-transducing outer segment region of the photoreceptor, photons are absorbed in a time-varying, spatially dependent fashion. Because the transduction event is spatially localized around the site of photon absorption, the spatiotemporal patterns of light absorption in outer segments are an important receiver input characteristic. This aspect of receptor biophysics has now been measured; the results were consistent with a theoretical model proposed for bleaching of a pigment in an unstirred layer.

THE ROD PHOTORECEPTORS IN VERTEBRATE eyes are oriented toward the incoming light (*1–3*). As a result, most of the light passes axially through the light-absorbing region, the rod outer segment (ROS). This feature, along with the highly organized ultrastructure of the ROS (*4*), plays an important role in rod function.

The ROS contains numerous rows of vesicular disks, in register. The disk membranes are packed with the photosensitive rhodopsin molecules. Although rhodopsin moves freely within the disk membranes (*5–8*), it does not "hop" from disk to disk (*5*).

C. L. Makino and T. P. Williams, Institute of Molecular Biophysics, Florida State University, Tallahassee, FL 32306.

L. N. Howard, Department of Mathematics, Florida State University, Tallahassee, FL 32306.

*To whom correspondence should be addressed at Department of Neurobiology, Sherman Fairchild Science Building, Stanford University School of Medicine, Stanford, CA 94305.

In a dark-adapted ROS, all disks contain the same concentration of rhodopsin (*9*). Axial passage of the light will bleach more pigment at the base, near the inner segment, than at the sclerad tip. Initially, the axial pattern of bleaching will show an exponential decrease, but because bleaching changes the light-filtering characteristics of the disk surfaces, the patterns of light absorption change with time in the light. This phenomenon can be demonstrated in single ROSs with microspectrophotometry.

The tropical toad *Bufo marinus* was used in this study because of the large size of its rods (6 by 60 μm ROSs were not uncommon). Toads were kept on a 12:12 light: dark cycle but were dark-adapted for 12 to 14 hours before use. During the final 30 minutes of dark adaptation, the toad was immersed in a 10% aqueous solution of MS-222 (Sandoz). The eyes were enucleated under dim red light, with care being taken to avoid disruption of the physiological optics. One eye from each animal was placed in Ringer solution (*10*), covered, and refrigerated. The other eye was exposed to a diffuse field of 500-nm monochromatic light (*11*) for several minutes. Then, the anterior segment was quickly removed, and 50 m*M* NH_2OH in Ringer solution was poured into the eyecup. After 2 to 4 minutes, the eyecup was transferred into 10 m*M* NH_2OH. The MS-222, the enucleation, and the hydroxylamine served to "freeze" the bleaching pattern in the ROSs by inhibiting rhodopsin regeneration (*12–14*) (the physiological mechanism whereby the animal restores its bleached rhodopsin to the prebleached state). Small pieces of retina were cut off and dabbed onto a polylysine-coated cover slip (*15*) to isolate single ROSs. The cover slip was encircled with silicone oil, and another, untreated cover slip was placed on top. This preparation was mounted onto the stage of a photon-counting, single-beam, MacNichol-type microspectrophotometer (*16*). With a 2 by 6 μm measuring beam, absorbance spectra were measured at various distances from the base of each outer segment.

After a light exposure, an ROS always contained less rhodopsin at its base than at its tip (Fig. 1). Measurements made on ROSs from the other eye, which had been kept in the dark, were used to estimate the dark-adapted concentrations of rhodopsin (c_0 values) in the light-exposed ROSs. This allowed the data to be expressed in terms of dimensionless numbers: the fraction of unbleached rhodopsin remaining versus normalized distance from the base (Fig. 2A). The observed, intracellular distributions of rhodopsin remaining were fitted with the relation (*17*) (Fig. 2, A and B):

$$\frac{c_l}{c_0} = \frac{\exp(\alpha c_0 l)}{[\exp(\alpha c_0 l) + \exp(\alpha\gamma I_0 t)] - 1} \quad (1)$$

where c_l is the concentration of rhodopsin at distance l from the base, α is the molar

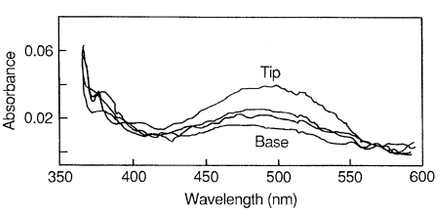

Fig. 1. Absorbance spectra from a bleached ROS. Each spectrum was measured at a different axial position in this ROS. The amplitude of each curve is proportional to the concentration of unbleached rhodopsin. The amplitude differences, which were most noticeable at 503 nm, the lambda max of rhodopsin, indicated that the rhodopsin concentration increased from base to tip. All curves approached a baseline level near 600 nm.